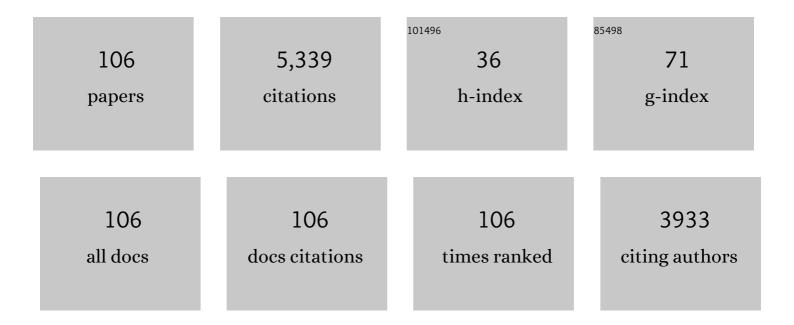
## Xiaohong Zhang

List of Publications by Year in descending order

Source: https://exaly.com/author-pdf/3718634/publications.pdf Version: 2024-02-01



#	Article	IF	CITATIONS
1	Instantaneous Real-Time Kinematic Decimeter-Level Positioning with BeiDou Triple-Frequency Signals over Medium Baselines. Sensors, 2016, 16, 1.	2.1	1,274
2	Precise positioning with current multi-constellation Global Navigation Satellite Systems: GPS, GLONASS, Galileo and BeiDou. Scientific Reports, 2015, 5, 8328.	1.6	264
3	Regional reference network augmented precise point positioning for instantaneous ambiguity resolution. Journal of Geodesy, 2011, 85, 151-158.	1.6	200
4	Multi-GNSS phase delay estimation and PPP ambiguity resolution: GPS, BDS, GLONASS, Galileo. Journal of Geodesy, 2018, 92, 579-608.	1.6	150
5	Initial assessment of the COMPASS/BeiDou-3: new-generation navigation signals. Journal of Geodesy, 2017, 91, 1225-1240.	1.6	149
6	Integrating GPS and GLONASS to accelerate convergence and initialization times of precise point positioning. GPS Solutions, 2014, 18, 461-471.	2.2	147
7	Assessment of precise orbit and clock products for Galileo, BeiDou, and QZSS from IGS Multi-GNSS Experiment (MGEX). GPS Solutions, 2017, 21, 279-290.	2.2	147
8	Quality assessment of GNSS observations from an Android N smartphone and positioning performance analysis using time-differenced filtering approach. GPS Solutions, 2018, 22, 1.	2.2	137
9	Modeling and assessment of triple-frequency BDS precise point positioning. Journal of Geodesy, 2016, 90, 1223-1235.	1.6	108
10	Satellite clock estimation at 1ÂHz for realtime kinematic PPP applications. GPS Solutions, 2011, 15, 315-324.	2.2	105
11	Timing group delay and differential code bias corrections for BeiDou positioning. Journal of Geodesy, 2015, 89, 427-445.	1.6	100
12	LEO constellation-augmented multi-GNSS for rapid PPP convergence. Journal of Geodesy, 2019, 93, 749-764.	1.6	93
13	Ambiguity resolved precise point positioning with GPS and BeiDou. Journal of Geodesy, 2017, 91, 25-40.	1.6	88
14	Realâ€ŧime highâ€rate coâ€seismic displacement from ambiguityâ€fixed precise point positioning: Application to earthquake early warning. Geophysical Research Letters, 2013, 40, 295-300.	1.5	87
15	Three-frequency BDS precise point positioning ambiguity resolution based on raw observables. Journal of Geodesy, 2018, 92, 1357-1369.	1.6	81
16	Improving the Estimation of Uncalibrated Fractional Phase Offsets for PPP Ambiguity Resolution. Journal of Navigation, 2012, 65, 513-529.	1.0	79
17	Clobal Ionospheric Modelling using Multi-GNSS: BeiDou, Galileo, GLONASS and GPS. Scientific Reports, 2016, 6, 33499.	1.6	73
18	Benefits of the third frequency signal on cycle slip correction. GPS Solutions, 2016, 20, 451-460.	2.2	68

#	Article	IF	CITATIONS
19	Generating GPS satellite fractional cycle bias for ambiguity-fixed precise point positioning. GPS Solutions, 2016, 20, 771-782.	2.2	64
20	Characteristics of inter-frequency clock bias for Block IIF satellites and its effect on triple-frequency GPS precise point positioning. GPS Solutions, 2017, 21, 811-822.	2.2	63
21	The contribution of Multi-CNSS Experiment (MGEX) to precise point positioning. Advances in Space Research, 2017, 59, 2714-2725.	1.2	59
22	Satellite availability and point positioning accuracy evaluation on a global scale for integration of GPS, GLONASS, BeiDou and Galileo. Advances in Space Research, 2019, 63, 2696-2710.	1.2	56
23	Surface Ice Flow Velocity and Tide Retrieval of the Amery Ice Shelf using Precise Point Positioning. Journal of Geodesy, 2006, 80, 171-176.	1.6	54
24	Improved precise point positioning in the presence of ionospheric scintillation. GPS Solutions, 2014, 18, 51-60.	2.2	54
25	Precise Point Positioning with Partial Ambiguity Fixing. Sensors, 2015, 15, 13627-13643.	2.1	52
26	Performance analysis of triple-frequency ambiguity resolution with BeiDou observations. GPS Solutions, 2016, 20, 269-281.	2.2	51
27	Performance Evaluation of Single-frequency Precise Point Positioning with GPS, GLONASS, BeiDou and Galileo. Journal of Navigation, 2017, 70, 465-482.	1.0	49
28	GPS inter-frequency clock bias estimation for both uncombined and ionospheric-free combined triple-frequency precise point positioning. Journal of Geodesy, 2019, 93, 473-487.	1.6	48
29	Performance evaluation of single-frequency point positioning with GPS, GLONASS, BeiDou and Galileo. Survey Review, 2017, 49, 197-205.	0.7	45
30	GPS + Galileo + BeiDou precise point positioning with triple-frequency ambiguity resolution. GF Solutions, 2020, 24, 1.	2.2 S	45
31	Performance evaluation of real-time global ionospheric maps provided by different IGS analysis centers. GPS Solutions, 2019, 23, 1.	2.2	44
32	Multipath extraction and mitigation for high-rate multi-GNSS precise point positioning. Journal of Geodesy, 2019, 93, 2037-2051.	1.6	43
33	Precise orbit determination for BDS3 experimental satellites using iGMAS and MGEX tracking networks. Journal of Geodesy, 2019, 93, 103-117.	1.6	42
34	Adaptive robust Kalman filtering for precise point positioning. Measurement Science and Technology, 2014, 25, 105011.	1.4	41
35	The improvement in integer ambiguity resolution with INS aiding for kinematic precise point positioning. Journal of Geodesy, 2019, 93, 993-1010.	1.6	41
36	Estimation and analysis of differential code biases for BDS3/BDS2 using iGMAS and MGEX observations. Journal of Geodesy, 2019, 93, 419-435.	1.6	39

#	Article	IF	CITATIONS
37	Multi-GNSS fractional cycle bias products generation for GNSS ambiguity-fixed PPP at Wuhan University. GPS Solutions, 2020, 24, 1.	2.2	38
38	Hybrid constellation design using a genetic algorithm for a LEO-based navigation augmentation system. GPS Solutions, 2020, 24, 1.	2.2	36
39	Ambiguity resolution in precise point positioning with hourly data for global single receiver. Advances in Space Research, 2013, 51, 153-161.	1.2	35
40	Assessment of correct fixing rate for precise point positioning ambiguity resolution on a global scale. Journal of Geodesy, 2013, 87, 579-589.	1.6	35
41	A Novel Method for Precise Onboard Real-Time Orbit Determination with a Standalone GPS Receiver. Sensors, 2015, 15, 30403-30418.	2.1	35
42	New optimal smoothing scheme for improving relative and absolute accuracy of tightly coupled GNSS/SINS integration. GPS Solutions, 2017, 21, 861-872.	2.2	34
43	Real-time clock jump compensation for precise point positioning. GPS Solutions, 2014, 18, 41-50.	2.2	32
44	lonospheric Total Electron Content Estimation Using GNSS Carrier Phase Observations Based on Zero-Difference Integer Ambiguity: Methodology and Assessment. IEEE Transactions on Geoscience and Remote Sensing, 2021, 59, 817-830.	2.7	32
45	A comprehensive analysis of satellite-induced code bias for BDS-3 satellites and signals. Advances in Space Research, 2019, 63, 2822-2835.	1.2	31
46	Considering Inter-Frequency Clock Bias for BDS Triple-Frequency Precise Point Positioning. Remote Sensing, 2017, 9, 734.	1.8	30
47	Improved PPP Ambiguity Resolution with the Assistance of Multiple LEO Constellations and Signals. Remote Sensing, 2019, 11, 408.	1.8	27
48	Assessment and Validation of Three Ionospheric Models (IRIâ€2016, NeQuick2, and IGS IM) From 2002 to 2018. Space Weather, 2020, 18, e2019SW002422.	1.3	26
49	Triple-frequency multi-GNSS reflectometry snow depth retrieval by using clustering and normalization algorithm to compensate terrain variation. GPS Solutions, 2020, 24, 1.	2.2	26
50	GPS inter-frequency clock bias modeling and prediction for real-time precise point positioning. GPS Solutions, 2018, 22, 1.	2.2	24
51	Differential Inter-System Biases Estimation and Initial Assessment of Instantaneous Tightly Combined RTK with BDS-3, GPS, and Galileo. Remote Sensing, 2019, 11, 1430.	1.8	23
52	Mapping topside ionospheric vertical electron content from multiple LEO satellites at different orbital altitudes. Journal of Geodesy, 2020, 94, 1.	1.6	23
53	BDS triple-frequency carrier-phase linear combination models and their characteristics. Science China Earth Sciences, 2015, 58, 896-905.	2.3	22
54	Investigating GNSS PPP–RTK with external ionospheric constraints. Satellite Navigation, 2022, 3, .	4.6	22

#	Article	IF	CITATIONS
55	A comparison of three widely used GPS triple-frequency precise point positioning models. GPS Solutions, 2019, 23, 1.	2.2	20
56	Walker: Continuous and Precise Navigation by Fusing GNSS and MEMS in Smartphone Chipsets for Pedestrians. Remote Sensing, 2019, 11, 139.	1.8	20
57	Assessment of long-range kinematic GPS positioning errors by comparison with airborne laser altimetry and satellite altimetry. Journal of Geodesy, 2007, 81, 201-211.	1.6	19
58	Predicting atmospheric delays for rapid ambiguity resolution in precise point positioning. Advances in Space Research, 2014, 54, 840-850.	1.2	19
59	Global Ionospheric Modeling Using Multi-GNSS and Upcoming LEO Constellations: Two Methods and Comparison. IEEE Transactions on Geoscience and Remote Sensing, 2022, 60, 1-15.	2.7	19
60	Analysis of Atmospheric and Ionospheric Variations Due to Impacts of Super Typhoon Mangkhut (1822) in the Northwest Pacific Ocean. Remote Sensing, 2021, 13, 661.	1.8	19
61	Single-epoch RTK performance assessment of tightly combined BDS-2 and newly complete BDS-3. Satellite Navigation, 2021, 2, .	4.6	18
62	Influence of the GLONASS inter-frequency bias on differential code bias estimation and ionospheric modeling. GPS Solutions, 2017, 21, 1355-1367.	2.2	17
63	Kalman-filter-based undifferenced cycle slip estimation in real-time precise point positioning. GPS Solutions, 2019, 23, 1.	2.2	17
64	Improving the Performance of Galileo Uncombined Precise Point Positioning Ambiguity Resolution Using Triple-Frequency Observations. Remote Sensing, 2019, 11, 341.	1.8	17
65	Daily Global Plasmaspheric Maps Derived From COSMIC GPS Observations. IEEE Transactions on Geoscience and Remote Sensing, 2014, 52, 6040-6046.	2.7	16
66	Multi-GNSS contributions to differential code biases determination and regional ionospheric modeling in China. Advances in Space Research, 2020, 65, 221-234.	1.2	16
67	Mitigation of Unmodeled Error to Improve the Accuracy of Multi-GNSS PPP for Crustal Deformation Monitoring. Remote Sensing, 2019, 11, 2232.	1.8	15
68	Influencing Factors of GNSS Differential Inter-System Bias and Performance Assessment of Tightly Combined GPS, Galileo, and QZSS Relative Positioning for Short Baseline. Journal of Navigation, 2019, 72, 965-986.	1.0	15
69	A method of improving ambiguity fixing rate for post-processing kinematic GNSS data. Satellite Navigation, 2020, 1, .	4.6	15
70	PPP-RTK considering the ionosphere uncertainty with cross-validation. Satellite Navigation, 2022, 3, .	4.6	15
71	Detection of ionospheric disturbances driven by the 2014 Chile tsunami using GPS total electron content in New Zealand. Journal of Geophysical Research: Space Physics, 2015, 120, 7918-7925.	0.8	14
72	Attitude variometric approach using DGNSS/INS integration to detect deformation in railway track irregularity measuring. Journal of Geodesy, 2019, 93, 1571-1587.	1.6	14

#	Article	IF	CITATIONS
73	Capturing coseismic displacement in real time with mixed single- and dual-frequency receivers: application to the 2018 Mw7.9 Alaska earthquake. GPS Solutions, 2019, 23, 1.	2.2	14
74	Estimation and analysis of multi-GNSS observable-specific code biases. GPS Solutions, 2021, 25, 1.	2.2	14
75	Impact of sampling rate of IGS satellite clock on precise point positioning. Geo-Spatial Information Science, 2010, 13, 150-156.	2.4	13
76	Influence of clock jump on the velocity and acceleration estimation with a single GPS receiver based on carrier-phase-derived Doppler. GPS Solutions, 2013, 17, 549-559.	2.2	13
77	Receiver Time Misalignment Correction for GPS-based Attitude Determination. Journal of Navigation, 2015, 68, 646-664.	1.0	13
78	High-precision coseismic displacement estimation with a single-frequency GPS receiver. Geophysical Journal International, 2015, 202, 612-623.	1.0	13
79	Performance of GNSS Global Ionospheric Modeling Augmented by LEO Constellation. Earth and Space Science, 2020, 7, e2019EA000898.	1.1	13
80	An enhanced foot-mounted PDR method with adaptive ZUPT and multi-sensors fusion for seamless pedestrian navigation. GPS Solutions, 2022, 26, 1.	2.2	12
81	Observation of ionospheric disturbances induced by the 2011 Tohoku tsunami using far-field GPS data in Hawaii. Earth, Planets and Space, 2015, 67, .	0.9	11
82	Precise Orbit Determination for LEO Satellites With Ambiguity Resolution: Improvement and Comparison. Journal of Geophysical Research: Solid Earth, 2021, 126, e2021JB022491.	1.4	11
83	Application of Collocated GPS and Seismic Sensors to Earthquake Monitoring and Early Warning. Sensors, 2013, 13, 14261-14276.	2.1	10
84	Tightly Combined BeiDou B2 and Galileo E5b Signals for Precise Relative Positioning. Journal of Navigation, 2017, 70, 1253-1266.	1.0	10
85	Topside Ionosphere of NeQuick2 and IRIâ€⊋016 Validated by Using Onboard GPS Observations From Multiple LEO Satellites. Journal of Geophysical Research: Space Physics, 2020, 125, e2020JA027999.	0.8	10
86	Common-mode error and multipath mitigation for subdaily crustal deformation monitoringÂwithÂhigh-rateÂGPS observations. GPS Solutions, 2021, 25, 1.	2.2	10
87	Electron Density Reconstruction by Ionospheric Tomography From the Combination of GNSS and Upcoming LEO Constellations. Journal of Geophysical Research: Space Physics, 2021, 126, e2020JA029074.	0.8	10
88	Evaluation of NTCM-BC and a proposed modification for single-frequency positioning. GPS Solutions, 2017, 21, 1535-1548.	2.2	8
89	A New Method for GNSS Multipath Mitigation with an Adaptive Frequency Domain Filter. Sensors, 2018, 18, 2514.	2.1	8
90	Global multiple tropopause features derived from COSMIC radio occultation data during 2007 to 2012. Journal of Geophysical Research D: Atmospheres, 2014, 119, 8515-8534.	1.2	7

#	Article	lF	CITATIONS
91	LEO Constellation-Augmented Multi-GNSS for 3D Water Vapor Tomography. Remote Sensing, 2021, 13, 3056.	1.8	7
92	Assessment of the performance of GPS/Galileo PPP-RTK convergence using ionospheric corrections from networks with different scales. Earth, Planets and Space, 2022, 74, .	0.9	7
93	Serverâ€Based Realâ€Time Precise Point Positioning and Its Application. Chinese Journal of Geophysics, 2010, 53, 372-379.	0.2	6
94	Performance enhancement for GPS positioning using constrained Kalman filtering. Measurement Science and Technology, 2015, 26, 085020.	1.4	5
95	Frequency design of LEO-based navigation augmentation signals for dual-band ionospheric-free ambiguity resolution. GPS Solutions, 2022, 26, 1.	2.2	5
96	Investigation on Horizontal and Vertical Traveling Ionospheric Disturbances Propagation in Global‣cale Using GNSS and Multi‣EO Satellites. Space Weather, 2022, 20, .	1.3	5
97	Modeling and Performance Analysis of GPS/GLONASS/BDS Precise Point Positioning. Lecture Notes in Electrical Engineering, 2014, , 251-263.	0.3	4
98	Estimating multi-frequency satellite phase biases of BeiDou using maximal decorrelated linear ambiguity combinations. GPS Solutions, 2019, 23, 1.	2.2	4
99	The Performance of Three-Frequency GPS PPP-RTK with Partial Ambiguity Resolution. Atmosphere, 2022, 13, 1014.	1.0	4
100	Evaluation and validation of various rapid GNSS global ionospheric maps over one solar cycle. Advances in Space Research, 2022, 70, 2494-2505.	1.2	4
101	A novel Stop&Go GPS precise point positioning (PPP) method and its application in geophysical exploration and prospecting. Survey Review, 2012, 44, 251-255.	0.7	3
102	A Multi-Step Multi-Order Numerical Difference Method for Traveling Ionospheric Disturbances Detection. Lecture Notes in Electrical Engineering, 2014, , 331-340.	0.3	3
103	Characterizing inter-frequency bias and signal quality for GLONASS satellites with triple-frequency transmissions. Advances in Space Research, 2019, 64, 1398-1414.	1.2	2
104	Integration of GNSS and Seismic Data for Earthquake Early Warning: A Case Study on the 2011 Mw 9.0 Tohoku-Oki Earthquake. Lecture Notes in Electrical Engineering, 2014, , 437-450.	0.3	2
105	Retrieval of Airborne Lidar Misalignments Based on the Stepwise Geometric Method. Survey Review, 2010, 42, 176-192.	0.7	1
106	Study on the Relationship Between the Equivalent GDOP and the Convergence Time of LEO-Augmented BDS PPP. Lecture Notes in Electrical Engineering, 2022, , 244-254.	0.3	1